X-612-67-580

NASA TM X-63046

INTERACTION OF THE MAGNETIZED SOLAR WIND WITH THE MOON

GPO PRICE $ _____

CFSTI PRICE(S) $ _____

Hard copy (HC) 3.00

Microfiche (MF) _____

ff 653 July 65

Y. C. WHANG

NOVEMBER 1967

GODDARD SPACE FLIGHT CENTER
GREENBELT, MARYLAND

INTERACTION OF THE MAGNETIZED SOLAR WIND WITH THE MOON

Y. C. Whang*

November 1967

Submitted to the Physics of Fluids for Publication.
Presented at American Physical Society, Division of Fluid Dynamics Meeting, November 21, 1967 at Lehigh University.

* National Academy of Sciences-National Research Council Senior Postdoctoral Research Associate, on leave from the Catholic University of America.

INTERACTION OF THE MAGNETIZED SOLAR WIND WITH THE MOON

Y. C. Whang*

Laboratory for Space Sciences
NASA-Goddard Space Flight Center
Greenbelt, Maryland 20771 U.S.A.

Abstract

In July 1967 the Explorer 35 spacecraft was launched into a lunar orbit to study the interaction of the magnetized solar wind plasma with the moon. The experimental results indicate that a detached bow shock wave does not exist in the vicinity of the moon. Thus the flow conditions near the moon do not resemble those near the earth's magnetosphere. In this paper the solar wind flow around the moon is treated theoretically as a free molecule flow of magnetized plasma. Analytical results are obtained to describe the distribution of the ion density and the ion flux in the vicinity of the moon. A sizable empty cavity is produced in the near-downstream vicinity of the moon; across the boundary of the cavity the plasma flow changes rapidly from the undisturbed condition to the void condition. The disturbed region in the downstream forms a long wake on the dark side of the moon. The direction of the wake is deflected slightly toward the field lines. The thickness of the wake, measured perpendicular to the plane of the solar wind velocity and the interplanetary magnetic field, is constant at one lunar diameter. On the other hand, the width of the wake, measured parallel to that plane, increases with distance from the moon. The length of the wake is of the order of 100 lunar radii.

1. Introduction

The solar wind [1,2] flows approximately radially outward from the sun in all directions continuously. It flows past the earth's orbit at a supersonic velocity. The solar magnetic lines of force are carried outward by the solar wind and are twisted into the form of Archimedean spirals. The earth's magnetosphere presents a blunt-nosed obstacle in the course of the solar wind blocking the motion of both the solar wind plasma and the interplanetary magnetic field lines. In the vicinity of the earth's magnetosphere, the solar wind plasma behaves as a continuum, and a detached bow shock wave is formed standing on the sunward side of the earth's magnetosphere. Satellite measurements [3,4] have detected the presence of the detached bow shock and the magnetosheath region between the magnetosphere and the bow shock. Theoretical calculations [5-7] have been successful in explaining the gross features and the overall shape of the interaction region. As the supersonic solar wind interacts with the moon, it might be expected that the flow conditions near the moon would resemble those near the earth's magnetosphere with a detached bow shock standing on the sunward side of the moon. On July 22, 1967 the NASA Explorer 35 spacecraft was placed into a lunar orbit to study the interaction of the solar wind with the moon, but no detached bow shock has been observed [8,9]. The experimental results indicate that the actual interaction of the solar wind with the moon is quite different from that of the solar wind with the earth.

In ordinary fluid mechanics, a division of fluid flows into various regimes is determined by the ratio of the collisional mean-free-path λ to the characteristic length of the flow L. In the

continuum flow regime, where $\lambda \ll L$, particle-particle interactions dominate over particle-surface interactions. In the free molecule flow regime, where $\lambda \gg L$, particle-surface interactions dominate over particle-particle interactions. Between these two limiting regimes is the transition flow regime. When a supersonic flow encounters a blunt-nosed obstacle, in the continuum flow regime a detached shock wave is generated upstream of the obstacle, while in the free molecule flow regime no shock wave can be formed in the vicinity of the obstacle. Absence of a detached bow shock in the vicinity of the moon indicates that the interaction of the solar wind plasma with the moon behaves like a free molecule flow rather than a continuum flow.

The collisional mean-free-path of the solar wind plasma near the earth's orbit is of the order of 1 AU. In lieu of interparticle collisions, the interplanetary magnetic field has the important effect of causing the solar wind plasma to behave as a continuum for the interaction between the solar wind and the earth's magnetosphere. Thus the interaction length must be small in comparison with the dimension of the earth's magnetosphere. The exact scale of this interaction length is not well understood yet. The diameter of the earth's magnetosphere is about 50 times that of the moon, which suggests that the small size of the obstacle is responsible for the absence of continuum phenomena near the moon. In addition to the difference in their sizes, their contrary responses to the impinging plasma and field lines also affect the flow patterns around

the moon and the earth's magnetosphere. Firstly, the blunt nose of the earth's magnetosphere is very effective in blocking the penetration of the interplanetary magnetic field lines. On the contrary, the experimental results[8] obtained from Explorer 35 indicate that the moon does not have an intrinsic magnetic field and the average electrical conductivity of the moon is very low, the impinging field lines appear to diffuse through the lunar body very rapidly. Secondly, all the charged particles striking on the moon are captured by the cold surface of the moon; they will be neutralized and then re-emitted as cold neutral particles. Whereas the blunt nose of the earth's magnetosphere bounces off all impinging solar wind particles.

In this paper, we will treat the motion of ion particles of the solar wind in the vicinity of the moon as a free molecule flow of magnetized plasma. The moon's surface will be considered as perfectly absorbing with respect to the impinging charged particles.

2. Analysis

Let us consider that in the undisturbed upstream flow the solar wind moves with a steady uniform velocity $\underset{\sim}{U}_o$ with respect to the center of the moon, and a steady uniform interplanetary magnetic field $\underset{\sim}{B}_o$ is carried with the solar wind (Fig. 1). The velocity of a charged particle in the upstream can be expressed as the vector sum of a guiding-center velocity $\underset{\sim}{V}_G$ and a Larmor motion velocity $\underset{\sim}{C}_\perp$. The component of the guiding-center velocity normal to the field lines is the electric drift, which is exactly the component of $\underset{\sim}{U}_o$ normal to $\underset{\sim}{B}_o$. All charged particles have the same electric drift

velocity, which means that the guiding-centers do not have thermal motion transverse to the field lines. The component of the guiding-center velocity parallel to the field can be expressed as the sum of a thermal velocity $\underset{\sim}{C}_{\parallel}$ and a mean mass flow velocity which is equal to the component of $\underset{\sim}{U}_o$ parallel to $\underset{\sim}{B}_o$. Thus we can express the guiding center velocity as composed of two parts: the mean mass flow velocity $\underset{\sim}{U}_o$ and a thermal motion velocity along the field lines $\underset{\sim}{C}_{\parallel}$ (Fig. 2):

$$\underset{\sim}{V}_G = \underset{\sim}{U}_o + \underset{\sim}{C}_{\parallel} \qquad (1)$$

Physically, this equation means that the guiding center of a charged particle is constrained to move along a magnetic line which is itself moving with a velocity $\underset{\sim}{U}_o$.

The ion particles are rapidly gyrating about the guiding center with a Lamor radius of the order of 80 km, which is only a small fraction of the moon's radius (Rm = 1738 km). In order to find the lowest order solution for the ion flow in the vicinity of the moon we approximate each ion particle by an artificial guiding-center particle [11,12]. A guiding-center particle is considered as a charged particle located at its guiding center, moving with its guiding-center velocity, and with the oscillation about the guiding center representing internal energy, magnetic moment, and angular momentum of the particle. A collection of artificial guiding-center particles behaves as a one-dimensional gas which has thermal motion only along the field lines.

Next we assume that the distribution function of this one-dimensional guiding-center gas is Maxwellian in the undisturbed upstream flow, namely,

$$f_G = \pi^{-\frac{1}{2}} n_o \alpha_{\parallel} \exp(-\alpha_{\parallel}^2 C_{\parallel}^2) \qquad (2)$$

Here $\alpha_{\parallel}^2 = m_i/(2k T_{\parallel})$, with the parallel temperature $T_{\parallel}$ defined by

$$k T_{\parallel}/2 = (1/n_o) \int_{-\infty}^{\infty} (mC_{\parallel}^2/2) f_G \, dC_{\parallel}$$

In the free molecule flow in the vicinity of the moon, the particle-surface interaction dominates over the particle-particle interaction. We make the additional assumption that when the solar wind plasma arrives in the vicinity of the moon, each guiding center particle continues to move with its initial guiding-center velocity along a straight-line path unless it is captured by the moon's cold surface. The guiding-center distribution function remains constant on each straight path. Inevitably, the magnetic and the electric fields will be slightly disturbed in the moon's wake region. The drifts due to non-uniformity of the disturbed fields are small compared with the initial guiding-center velocity, and these "first-order" drifts are negligible in a "zero-order" solution.

Based on the assumptions outlined above, we can now calculate the ion density and the ion flux in the vicinity of the moon. We will choose a coordinate system moving with the center of the moon, with its origin located at the moon's center, the X-axis parallel to the velocity vector $\underset{\sim}{U}_o$, and the Z-axis along the direction of

$\underset{\sim}{B}_o \times \underset{\sim}{U}_o$ (Fig. 1). The scale of the coordinate system is normalized by using the moon's radius as a unit length. $\emptyset$ denotes the direction angle of the interplanetary magnetic field. $\underset{\sim}{e}_x$ and $\underset{\sim}{e}_1$ denote the unit vectors along the X-direction and the $\underset{\sim}{B}_o$-direction respectively.

The XY-plane which is parallel to both the solar wind velocity $\underset{\sim}{U}_o$ and the interplanetary magnetic field $\underset{\sim}{B}_o$ is a plane of symmetry for the flow around the moon. The guiding-center velocity has no component along the Z-direction. Thus the motion of each guiding-center particle is restricted on a Z=constant plane. The moon's surface would not intercept any guiding-center particle's trajectory in the region $|Z| > 1$, the flow field is undisturbed in this region. In the region $|Z| \leq 1$, we may first draw a line on the Z= constant plane tangential to the moon's surface on its upstream side (Fig. 3). At any point on the upstream side of this line, we can find guiding-center particles distributed over the whole spectrum of thermal velocity (i.e., $-\infty < C_{\parallel} < +\infty$), the flow field is not disturbed due to the presence of the moon. The ion density is n_o and the ion flux is $n_o \underset{\sim}{U}_o$ in the undisturbed region. The flow in the downstream side of the first tangential line is more or less disturbed.

If we draw a second line on the Z=constant plane tangential to the moon on its downstream side, we can divide the disturbed flow into the three regions identified as region I, II and III in Fig. 3. At any point $P(\underset{\sim}{r})$ in the disturbed region, the ion density and the ion flux can be calculated if the guiding center distribution function is known at that point as a function of $C_{\parallel}$. When an un-intercepted particle arrives at P, it still moves with its initial

$\underset{\sim}{U}_o$ and $C_{\parallel}$, and carries the same Maxwelliam distribution function f_G with it. Because the moon's surface behaves as a perfectly absorbing surface with respect to charged particles, no particle can arrive at point P if its straight-line trajectory has been intercepted by the moon's surface. Therefore at point P the guiding-center distribution function is Maxwellian in a certain interval in the one-dimensional $C_{\parallel}$ -space, and is zero outside of this interval. Let I_j denote the interval of $C_{\parallel}$ in region j within which the distribution function is Maxwellian. We can express these intervals as

$$\left.\begin{aligned} &I_1: (-\infty, -\gamma_1 U_o) \\ &I_2: (\gamma_2 U_o, +\infty) \\ &I_3: (-\infty, -\gamma_1 U_o) \text{ and } (\gamma_2 U_o, \infty) \end{aligned}\right\} \quad (3)$$

where
$$\gamma_1 = \sin(\alpha + \beta)/\sin(\phi - \alpha - \beta)$$
$$\gamma_2 = \sin(\alpha - \beta)/\sin(\phi + \alpha - \beta)$$
$$\alpha = \arcsin((1 - Z^2)^{\frac{1}{2}}(X^2 + Y^2)^{-\frac{1}{2}})$$
$$\beta = \arctan(Y/X)$$

Now the guiding-center distribution function in the disturbed regions (regions I, II and III) can be expressed as

$$\left.\begin{aligned} f_G &= \pi^{-\frac{1}{2}} n_o \alpha_{\parallel} \exp(-\alpha_{\parallel}^2 C_{\parallel}^2) \quad \text{for } C_{\parallel} \in I_j \\ &= 0 \quad \text{for } C_{\parallel} \notin I_j \end{aligned}\right\} \quad (4)$$

The ion density, n_o, and the ion flux, $n\underset{\sim}{u}$, can be calculated from

$$n = \int_{I_j} f_G \, dC_{\parallel} \quad (5)$$

and
$$n\underset{\sim}{u} = \int_{I_j} (\underset{\sim}{U}_o + \underset{\sim}{C}_{\parallel}) f_G \, dC_{\parallel} \quad (6)$$

Let $S = U/(2kT_{\parallel}/m_i)^{\frac{1}{2}}$ denote the so-called "speed ratio" in the free molecule flow regime. The integration, from (5) and (6), yields the following forms:

In region I,

$$\left.\begin{aligned} n/n_o &= (\tfrac{1}{2})\ \mathrm{erfc}(\gamma_1 S) \\ n\underset{\sim}{u}/(n_o U_o) &= (\tfrac{1}{2})\left[\underset{\sim}{e}_x\ \mathrm{erfc}\ (\gamma_1 S) - \underset{\sim}{e}_1 \exp\ (-\gamma_1{}^2 S^2)/(\pi^{\frac{1}{2}} S)\right] \end{aligned}\right\} (7)$$

In region II,

$$\left.\begin{aligned} n/n_o &= (1/2)\ \mathrm{erfc}\ (\gamma_2 S) \\ n\underset{\sim}{u}/(n_o U_o) &= (\tfrac{1}{2})\left[\underset{\sim}{e}_x\ \mathrm{erfc}\ (\gamma_2 S) + \underset{\sim}{e}_1 \exp\ (-\gamma_2^2 S^2)/(\pi^{\frac{1}{2}} S)\right] \end{aligned}\right\} (8)$$

In region III,

$$\left.\begin{aligned} n/n_o &= (\tfrac{1}{2})\ [\mathrm{erfc}\ (\gamma_1 S) + \mathrm{erfc}\ (\gamma_2 S)] \\ n\underset{\sim}{u}/(n_o U_o) &= (\tfrac{1}{2})\ \underset{\sim}{e}_x\ [\mathrm{erfc}\ (\gamma_1 S) + \mathrm{erfc}\ (\gamma_2 S)] - \\ &\quad \underset{\sim}{e}_1\ [\exp\ (-\gamma_1{}^2 S^2) - \exp\ (-\gamma_2{}^2 S^2)]/(2\pi^{\frac{1}{2}} S) \end{aligned}\right\} (9)$$

$\mathrm{Erfc}(\xi)$ is the complementary error function of ξ defined as

$$\mathrm{erfc}(\xi) = 1 - \mathrm{erf}\ (\xi)$$

$$= \frac{2}{\sqrt{\pi}} \int_{\xi}^{\infty} e^{-t^2}\, dt$$

3. Results

At the earth's orbit, the typical interplanetary conditions of the past few years directly observed from space satellites are of the order of $U \sim 400$ km/sec, $T \sim 10^5\ ^{o}K$, $n \sim 5$ ions/cm, $B \sim 6\gamma$ and $\phi \sim 135^{o}$ or 315^{o}. The temperature parallel to the magnetic field, $T_{\parallel}$, is about twice the temperature transverse to the magnetic field, $T_{\perp}$[13]. Based on these values some numerical computations have been carried out.

We shall first discuss the ion flux distribution. Fig. 4 shows the distribution of ion flux on the XY-coordinate plane for S=5 and $\phi = 90^{o}$, 105^{o}, 120^{o}, 135^{o} and 150^{o}. The guiding-center particles are insensitive to the polarity of the field line; when $\phi = \phi_1 + 180^{o}$ the flow pattern is exactly the same as that with $\phi = \phi_1$. The ion flux is disturbed mainly downstream from the moon. A sizable empty cavity is produced in the near-downstream vicinity of the moon; across the constant flux contours around the cavity the ion flux changes rapidly from the undisturbed condition to the void condition. A long wake is formed on the dark side of the moon. These features agree with the observations reported in references 9 and 14. When the field lines are perpendicular to the direction of the relative velocity of the solar wind, the wake region is relatively short; the length of the wake region increases as the acute angle between the two directions decreases. As ϕ tends to 180^{o}, the shape of the empty cavity approaches a circular cylinder with a radius of 1 R_m; the ion flux and the ion density are undisturbed outside the cylinder and zero inside. Fig. 5 plots the distribution of ion flux on the XY-coordinates plane for $\phi = 135^{o}$ and S = 3, 7 and 10. It is seen that the moon's wake becomes narrower and longer as the speed ratio S increases.

Let θ denote the angle between the direction of the ion flux and that of the solar wind velocity with respect to the moon,

$$\theta = \arctan (u_y/u_x).$$

The constant θ contours are plotted in Fig. 6 to show the change of ion flux direction in the moon's wake for typical interplanetary conditions,

S=7 and ϕ=135°. It should be noted that throughout this paper, angles are measured from the X-axis, the direction of the relative velocity of the solar wind with respect to the moon. In general the X-direction is slightly deflected from the sun-moon line; the deflection angle is determined by the following two factors: (1) The direction of the solar wind is not strictly along the heliocentric radial direction; the deviation from radial direction may be as large as 10°, the average direction of the solar wind[15,16] is from east of the sun by 1.5°. (2) The moon is orbiting around the sun with a velocity of 30 $\pm$ 1 km/sec, and must be included in calculating the relative velocity of the solar wind with respect to the moon. This latter effect is the aberration of the solar wind flow which is generally between 3-6°.

The direction of the wake is "steered" by both the solar wind velocity and the imbedded field lines. When ϕ = 90° or 180°, the flow is symmetrical about the XZ-plane, and the direction of the wake coincides with that of the upstream solar wind velocity with respect to the moon. From Figs. 4 and 5 we can see that when ϕ is between 90° and 180° the wake is deflected slightly toward the direction of the imbedded field lines. As the speed ratio S increases the steering of the wake direction becomes more dominantly controlled by the solar wind velocity.

A perspective view of the moon's wake is plotted in Fig. 7 to show the ion flux distribution over cross-sections X = 3,6,9,12 and 15. We can see that the flow is symmetrical about the XY-plane which is parallel to both the solar wind velocity, $\underset{\sim}{U}_o$, and the interplanetary magnetic field $\underset{\sim}{B}_o$. The thickness of the wake, measured perpendicular to the plane of symmetry, remains constant at one lunar diameter everywhere. The width of the wake measured in the plane of symmetry increases

as its distance from the moon increases. This shows the important role the interplanetary magnetic field plays in affecting the flow conditions in this wake region. In the absence of the magnetic field, we would see a wake flow symmetrical about the X-axis downstream of a sphere rather than a deflected wake symmetrical about the XY-plane.

The ion flux is of primary importance, because this is the quantity that can be directly measured from space satellites.[9] The distribution of ion density is useful in computing the electron flow and the magnetic field in the moon's vicinity. Since the direction of the forces between charged particles is such as to try to restore neutrality, it is characteristic of plasma to try to remain as electrically neutral as possible. The ion density distribution acts as a background for the electron flow in the moon's wake, and the electron density can deviate from the ion density only very slightly.

Finally we shall discuss the distribution of ion density in the vicinity of the moon. Figs. 8 and 9 show the ion density distribution compared with the ion flux distribution. The constant density contours are quite close to the constant flux contours, and thus the general feature of the moon's wake does not change whether we are dealing with the density or the flux.

As to the length of the wake, this author does not attempt to define it precisely. A typical variation of ion density and ion flux along the X-axis is given in Table 1. From this table it may be stated that the length of the moon's wake is of the order of 100 lunar radii.

Summary

As the solar wind interacts with the moon, the motion of ion particles in the vicinity of the moon is considered as a free molecule flow of guiding-center particles. Analytical results are obtained to describe the distribution of the ion density and the ion flux in the vicinity of the moon.

The interplanetary magnetic field has a strong effect on the flow of the magnetized solar wind plasma. The flow condition is symmetrical about a plane passing through the center of the moon and parallel to both the solar wind velocity and the imbedded field lines. A sizable empty cavity is produced in the near-downstream vicinity of the moon. The disturbed flow forms a long slightly curved and deflected wake on the darkside of the moon. The thickness of the wake, measured perpendicular to the plane of symmetry, remains constant at one lunar diameter. The width of the wake measured in the plane of symmetry, increases with its distance from the moon. The direction of the wake essentially follows that of the solar wind velocity with respect to the moon; it is also steered by the field lines to bend slightly toward the direction of the field lines. As the speed ratio increases the deflection angle decreases, and the steering of the wake direction becomes more dominantly controlled by the solar wind velocity. The length of the wake is of the order of 100 lunar radii.

Acknowledgments

The author gratefully acknowledges the fruitful discussions, suggestions, and support from Dr. Norman F. Ness. He is also grateful to Dr. Harold E. Taylor and Mr. Kenneth W. Behannon for valuable comments in reviewing the manuscript.

TABLE 1

Variation of ion density and ion flux along X-Axis (for $S = 5$ and $\phi = 135^{\circ}$)

X	n/n_o	$nu/n_o U_o$
25.0	0.68849	0.68801
50.0	0.84139	0.84133
75.0	0.89390	0.89388
100.0	0.92033	0.92032
125.0	0.93623	0.93623
150.0	0.94684	0.94684
175.0	0.95443	0.95443
200.0	0.96012	0.96012
225.0	0.96455	0.96455
250.0	0.96809	0.96809
275.0	0.97099	0.97099
300.0	0.97341	0.97341
325.0	0.97545	0.97545
350.0	0.97721	0.97721
375.0	0.97873	0.97873
400.0	0.98005	0.98005

References and Footnotes

* National Academy of Sciences - National Research Council Senior Postdoctoral Research Associate, on leave from the Catholic University of America.

1. R. J. Mackin, Jr. and M. Neugebauer, The Solar Wind (Pergamon Press, New York, 1966).
2. E. N. Parker, Interplanetary Dynamical Processes (Interscience Publishers, New York, 1963).
3. N. F. Ness, C. S. Scearce and J. B. Seek, J. Geophys. Res. 69, 3531 (1964).
4. H. Bridge, S. Egidi, A. Lazarus, E. Lyon and L. Jacobson, Space Res. 5, 969 (1965).
5. W. I. Axford, J. Geophys. Res. 67, 3791 (1962).
6. P. J. Kellogg, J. Geophys. Res. 67, 3805 (1962).
7. J. R. Spreiter, A. L. Summers and A. Y. Alksne, Planet. Space Sci. 14, 223 (1966).
8. N. F. Ness, K. W. Behannon, C. S. Scearce and S. C. Canterano, J. Geophys. Res. 72, (December, 1967).
9. E. F. Lyon, H. S. Bridge and J. H. Binsack, "Explorer 35 Plasma Measurements in the Vicinity of the Moon", Center for Space Research, MIT, CSR TR-67-7 (1967).
10. S. A. Schaaf, "Mechanics of Rarefied Gases" in Handbuch der Physik, edited by S. Flügge (Springer-Verlag, Berlin, 1963), Vol. VIII.
11. H. Grad, "A Guiding Center Fluid", AEC Report TID-7503, p. 495 (February 1956).

12. H. Grad, in Proceedings of the Symposium on Electromagnetices and Fluid Dynamics of Geseous Plasma (Polytechnic Institute of Brooklyn, New York 1961), p. 37.

13. A. J. Hundhausen, S. J. Bame, and N. F. Ness, J. Geophys. Res. 72, 5265, (1967).

14. N. F. Ness, J. Geophys. Res. 70, 517 (1965).

15. A. J. Hundhausen, J. R. Asbridge, S. J. Bame, and I. B. Strong, J. Geophys. Res. 72, 1979 (1967).

16. J. H. Wolfe, R. W. Silva, D. D. McKibbin, and R. H. Mason, J. Geophys. Res. 71, 3329 (1966).

FIGURE CAPTIONS

Figure 1 The coordinate system.

Figure 2 The guiding-center velocity vector and the guiding-center distribution function.

Figure 3 Three different regions in the disturbed flow.

Figure 4 The distribution of ion flux in the XY-coordinate plane for varying direction angle $\emptyset$.

Figure 5 The distribution of ion flux in the XY-coordinate plane for varying speed ratio S.

Figure 6 The direction of ion flux in the moon's wake. (The shaded areas indicate the magnitude of ion flux).

Figure 7 A perspective view of the moon's wake (for S=5, $\emptyset = 135^{o}$).

Figure 8 A comparison of the ion density distribution and the ion flux distribution.

Figure 9 A comparison of the ion density distribution and the ion flux distribution.

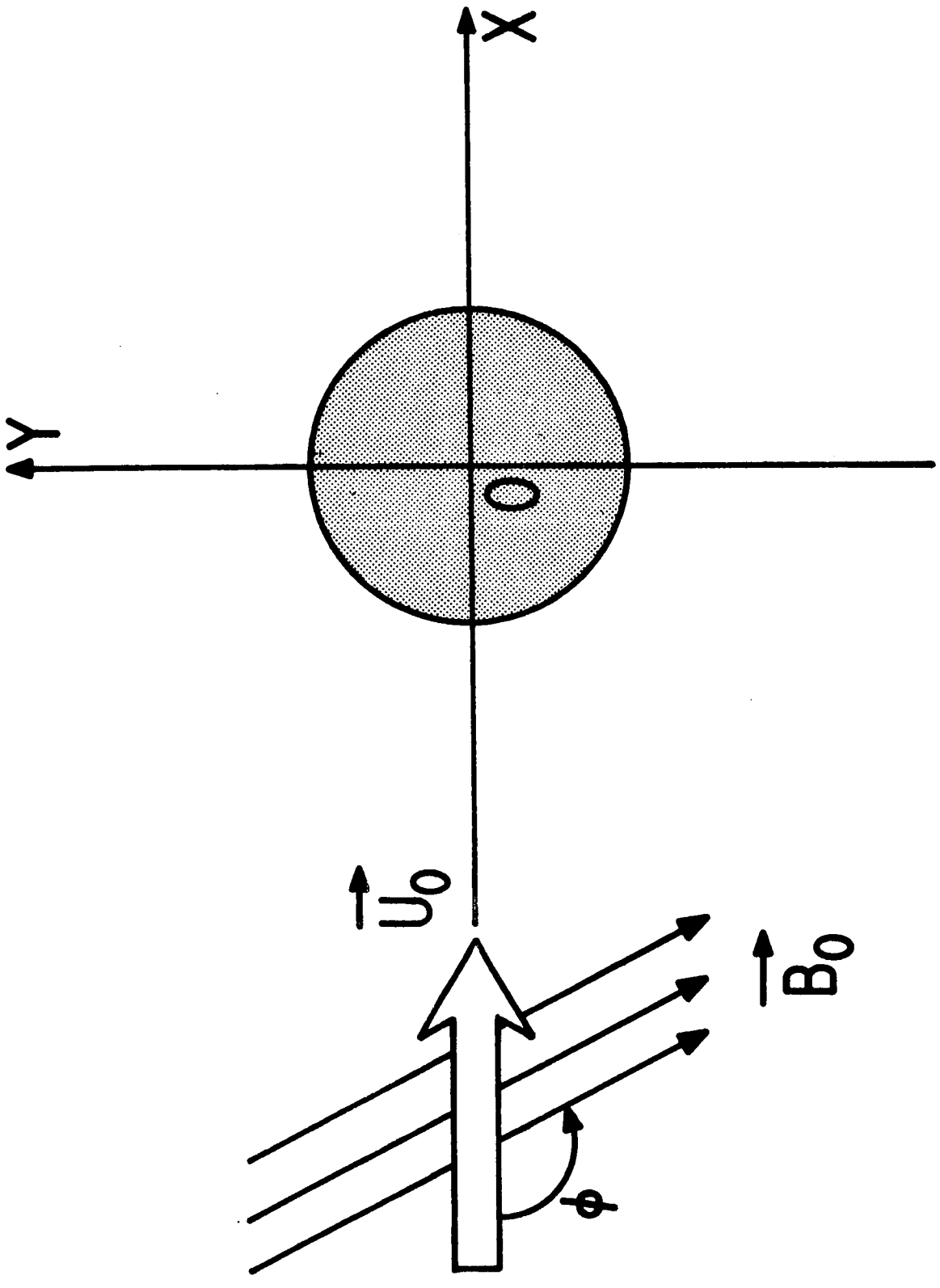

FIG. 1

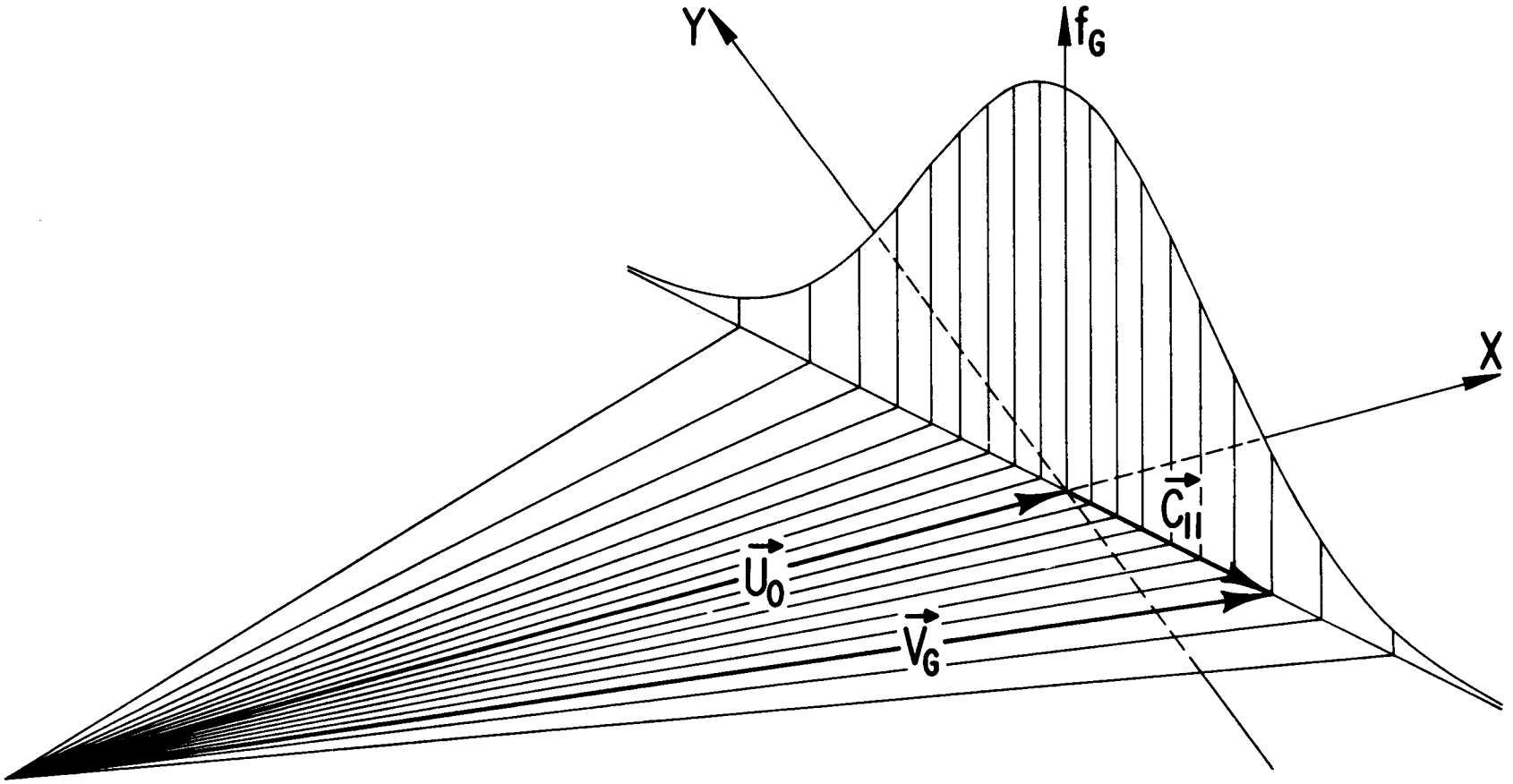

FIG. 2

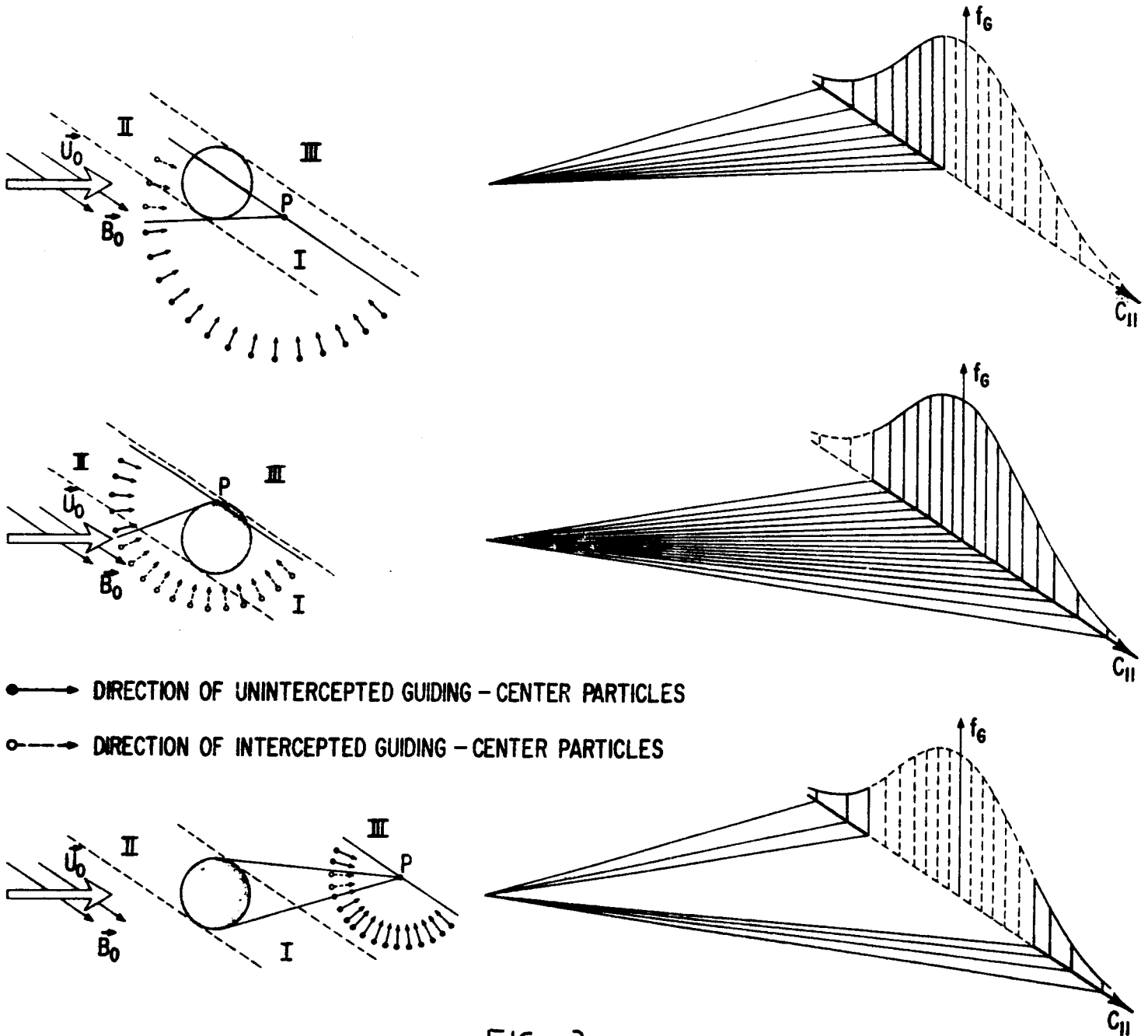
II
III
$\vec{U}_0$
P
$\vec{B}_0$
I
f_G
C_{II}
II
III
$\vec{U}_0$
P
$\vec{B}_0$
I
f_G
C_{II}
DIRECTION OF UNINTERCEPTED GUIDING - CENTER PARTICLES
DIRECTION OF INTERCEPTED GUIDING - CENTER PARTICLES
II
III
$\vec{U}_0$
P
$\vec{B}_0$
I
f_G
C_{II}

FIG. 3

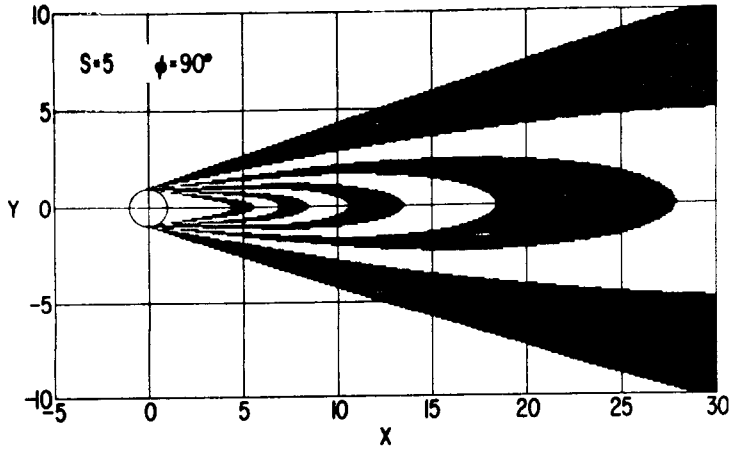
S=5 ϕ=90°
Y
X

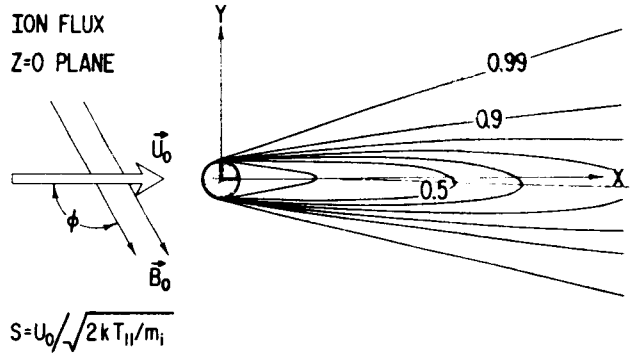
ION FLUX
Z=0 PLANE
$\vec{U}_0$
$\vec{B}_0$
ϕ
Y
X
0.99
0.9
0.5
$S=U_0/\sqrt{2kT_{||}/m_i}$

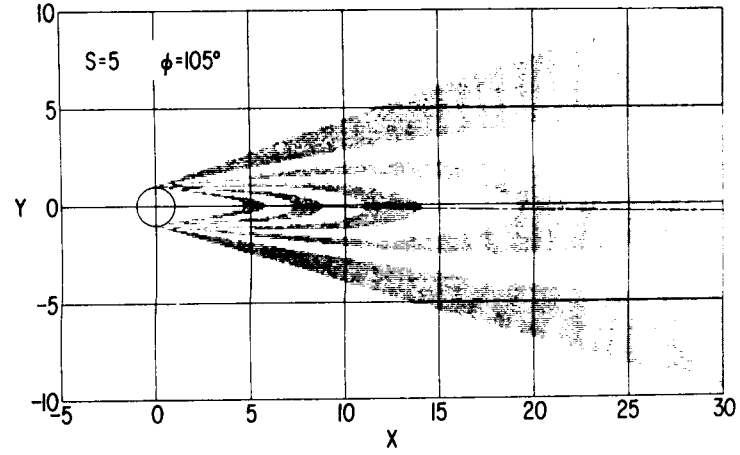
S=5 ϕ=105°
Y
X

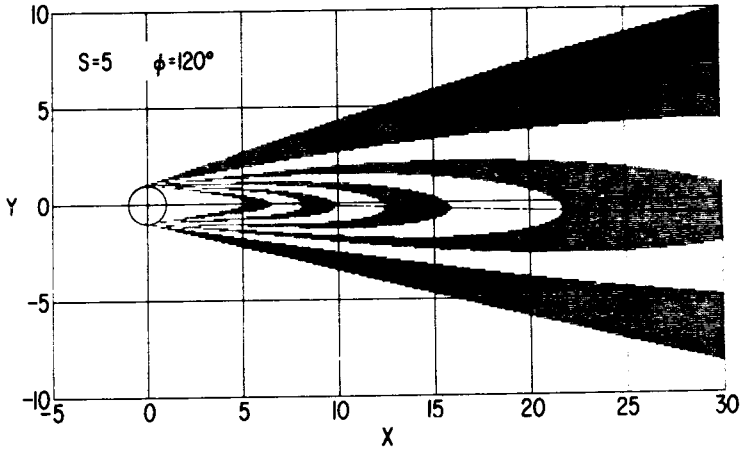
S=5 ϕ=120°
Y
X

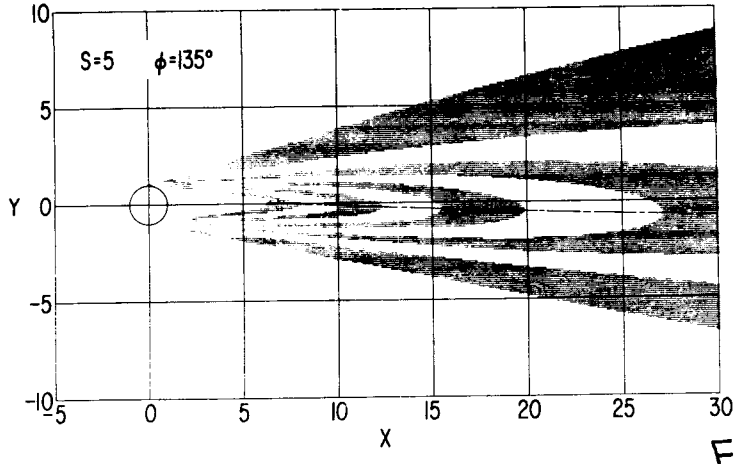
S=5 ϕ=135°
Y
X

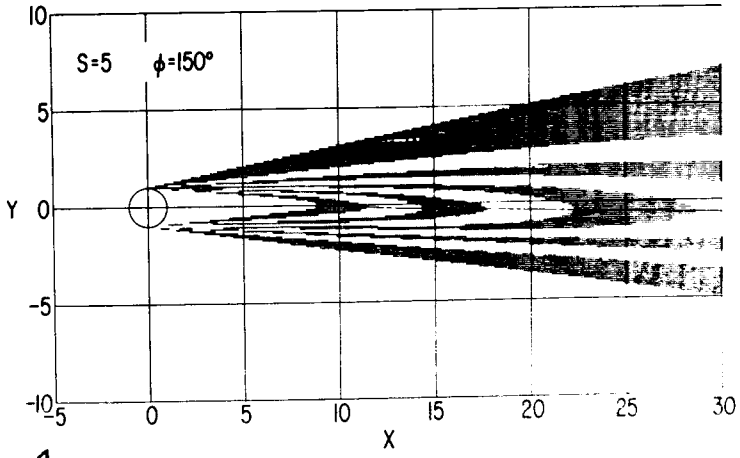
S=5 ϕ=150°
Y
X

FIG 4

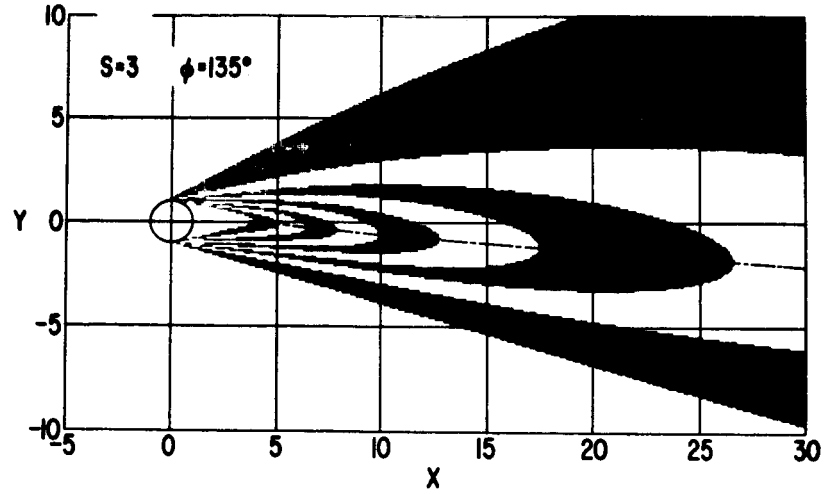
S=3 φ=135°
10
5
0
-5
-10
Y
-5
0
5
10
15
20
25
30
X

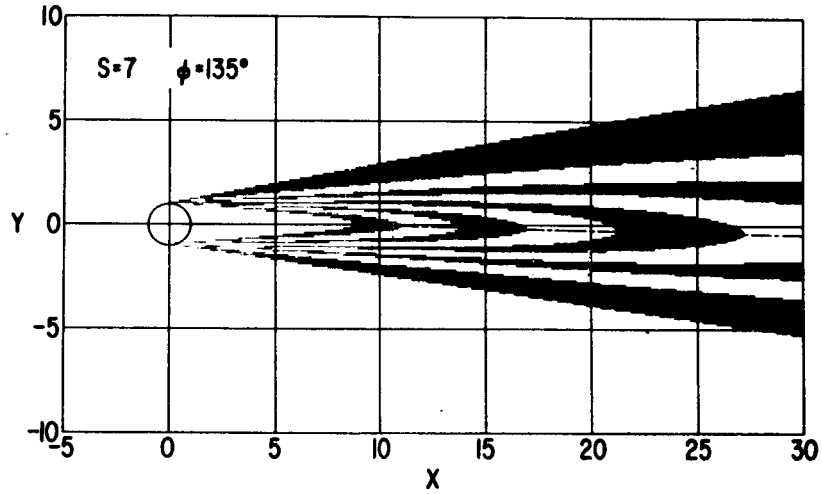
S=7 φ=135°
10
5
0
-5
-10
Y
-5
0
5
10
15
20
25
30
X

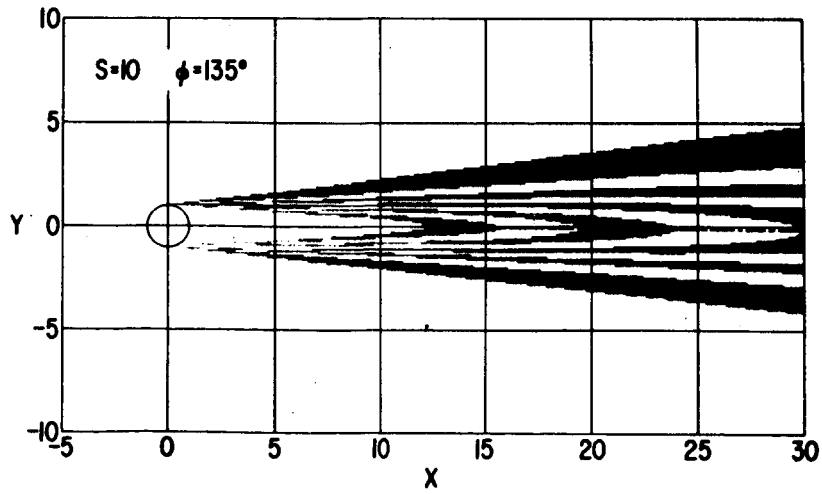
S=10 φ=135°
10
5
0
-5
-10
Y
-5
0
5
10
15
20
25
30
X

FIG 5

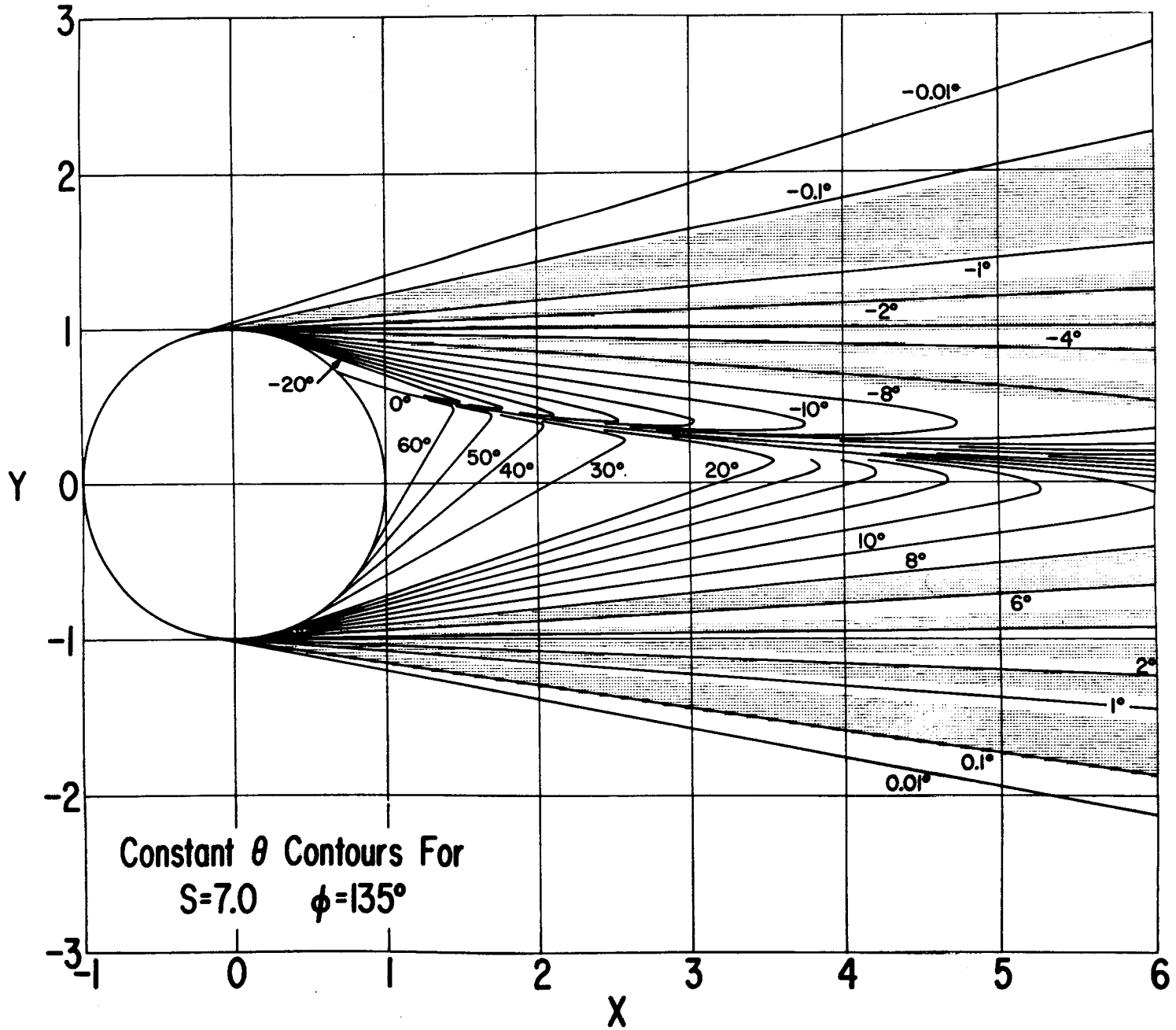
-0.01°
-0.1°
-1°
-2°
-4°
-8°
-10°
-20°
0°
60°
50°
40°
30°
20°
10°
8°
6°
2°
1°
0.1°
0.01°
Constant θ Contours For
S=7.0 φ=135°
Y
X
3
2
1
0
-1
-2
-3
-1
0
1
2
3
4
5
6

FIG 6

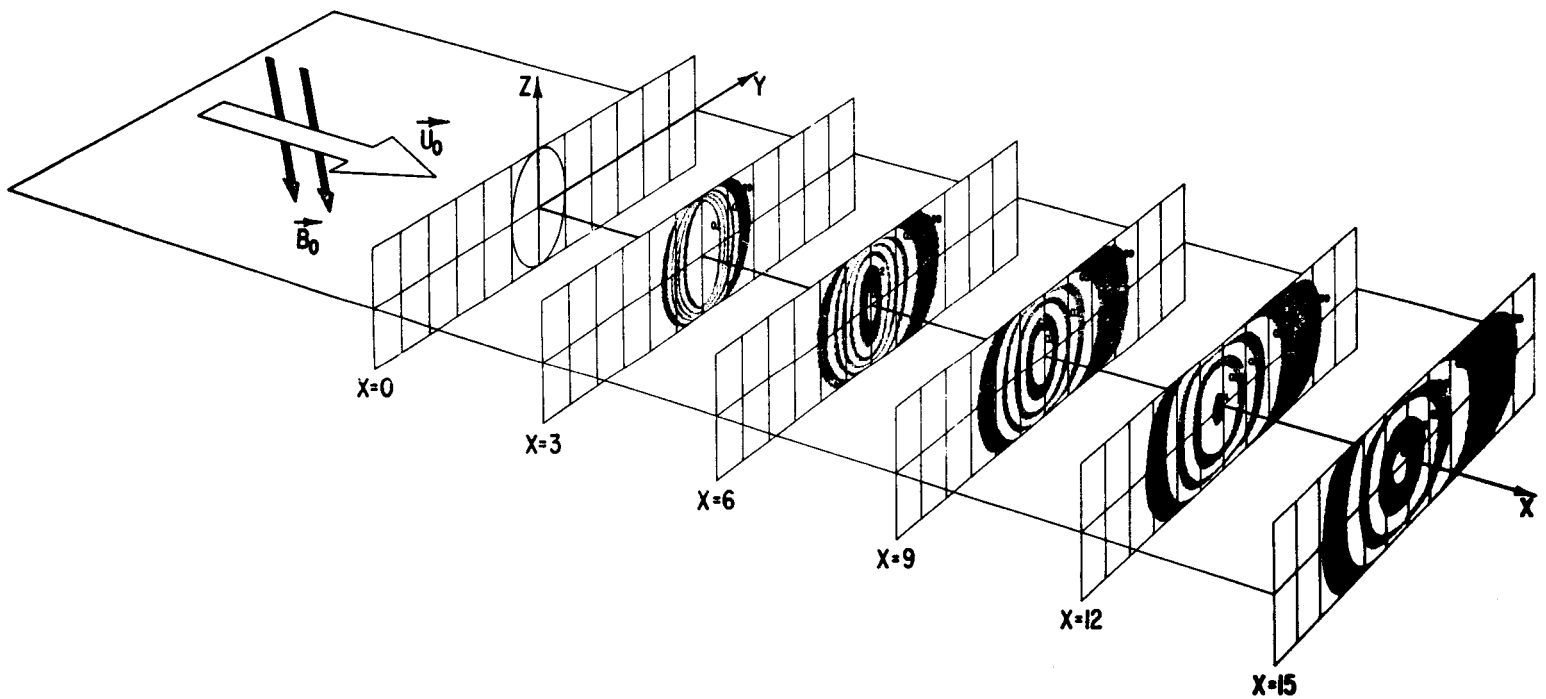

FIG 7

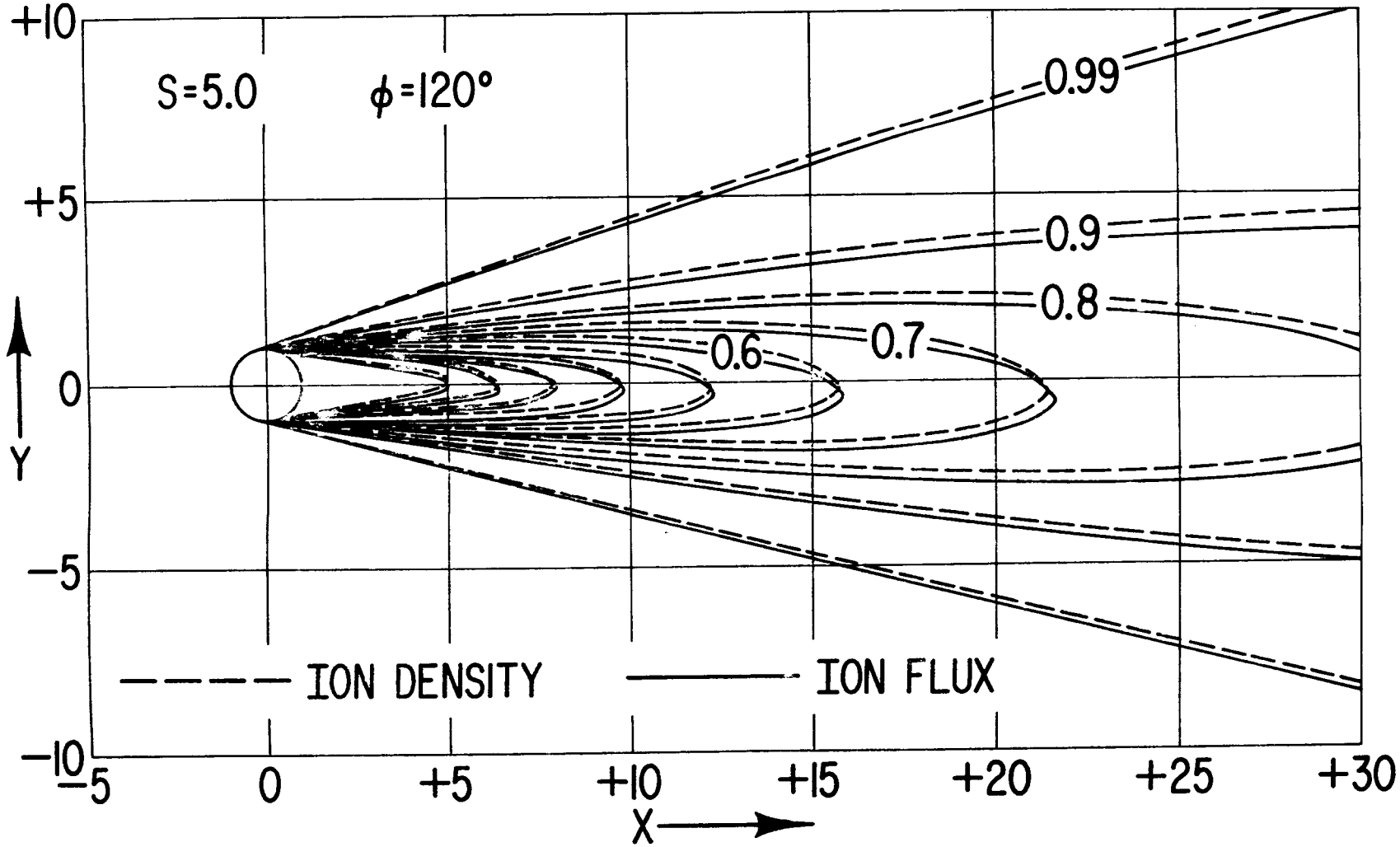
S=5.0
φ=120°
0.99
0.9
0.8
0.7
0.6
ION DENSITY
ION FLUX
+10
+5
0
−5
−10
Y
−5
0
+5
+10
+15
+20
+25
+30
X

FIG. 8

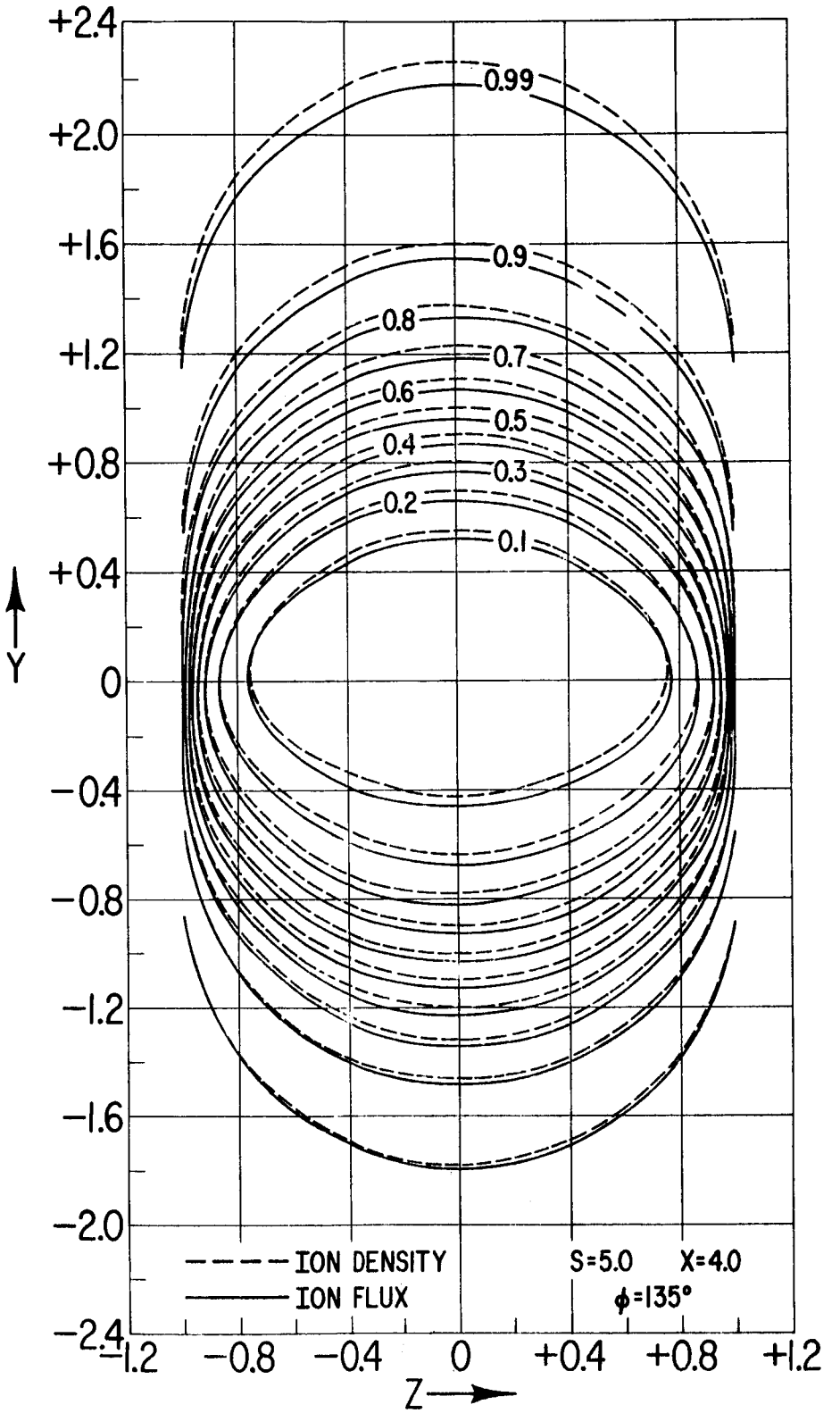
+2.4
+2.0
+1.6
+1.2
+0.8
+0.4
0
−0.4
−0.8
−1.2
−1.6
−2.0
−2.4
Y
0.99
0.9
0.8
0.7
0.6
0.5
0.4
0.3
0.2
0.1
ION DENSITY
ION FLUX
S=5.0 X=4.0
φ=135°
−1.2 −0.8 −0.4 0 +0.4 +0.8 +1.2
Z

FIG 9.